Published in final edited form as:

Mamm Genome. 2017 December ; 28(11-12): 465–475. doi:10.1007/s00335-017-9716-5.

Whole exome sequencing reveals a functional mutation in the GAIN domain of the Bai2 receptor underlying a forward mutagenesis hyperactivity QTL

David J. Speca[1], **James S. Trimmer**[2,3], **Andrew S. Peterson**[4], and **Elva Díaz**[1]

[1]Department of Pharmacology, University of California, Davis, CA, 95616

[2]Department of Neurobiology, Physiology and Behavior, University of California, Davis, CA, 95616

[3]Department of Physiology and Membrane Biology, University of California, Davis, CA, 95616

[4]Department of Molecular Biology, Genentech, South San Francisco, California 94080

Abstract

The identification of novel genes underlying complex mouse behavioral traits remains an important step in understanding normal brain function and its dysfunction in mental health disorders. To identify dominant mutations that influence locomotor activity, we performed a mouse *N*-ethyl-*N*-nitrosourea (ENU) forward mutagenesis screen and mapped several loci as quantitative traits. Here we describe the fine mapping and positional cloning of a hyperactivity locus mapped to the medial portion of mouse chromosome four. We employed a modified recombinant progeny testing approach to fine-map the confidence interval from ≈20 Mb down to ≈5 Mb. Whole exome resequencing of all exons in this region revealed a single missense mutation in the adhesion G protein-coupled receptor Brain specific angiogenesis inhibitor 2 (*Bai2*). This mutation, R619W, is located in a critical extracellular domain that is a hotspot for mutations in this receptor class. We find that in two different mammalian cell lines, surface expression of Bai2 R619W is markedly reduced relative to wild-type Bai2, suggesting that R619W is a loss-of-function mutation. Our results highlight the powerful combination of ENU mutagenesis and next generation sequencing to identify specific mutations that manifest as subtle behavioral phenotypes.

Keywords

Bai2; *Adgrb2*^{m1Djs}; *Adgrb2*$^{tm1b(KOMP)Mbp}$; QTL; ENU mutagenesis; GAIN domain; International Mouse Phenotyping Consortium (IMPC)

Introduction

Forward mutagenesis approaches in model organisms have been invaluable in elucidating the molecular underpinnings of many biological processes. Previously, we performed an ENU forward mutagenesis screen in mice in an effort to identify gene products that disrupt

Corresponding author: David J. Speca, Tel: (510) 333-0934, Fax: (530) 752-7710, djspeca@ucdavis.edu.

Conflicts of interest: The authors declare that no competing interests exist.

dopaminergic homeostasis (Speca et al. 2006). To enrich for mutations in the dopamine pathway, we utilized mice that were heterozygous for a null mutation in the dopamine transporter (DAT) as a sensitized background. Random ENU mutations were introduced into the germline on this background, and we phenotyped mutagenized animals for increased locomotor activity in a novel environment, in the hope of recapitulating the striking hyperactivity exhibited by DAT homozygous knockout animals (Giros et al. 1996). However, instead of finding strong enhancers with Mendelian inheritance patterns (and relatively facile genetic mapping), we identified numerous mouse pedigrees with subtle, yet heritable increases in locomotor activity. We used a quantitative trait locus (QTL) mapping approach to map locations of these heritable mutations, and surprisingly, we found that for the two pedigrees that we mapped, each pedigree harbored more than one significant QTL (Speca et al. 2006). Furthermore, some of the QTLs were dependent on the sensitized DAT background whereas others acted independent of the DAT, as semi-dominant traits (Speca et al. 2006).

Here we describe the fine-mapping, sequence identification, and preliminary characterization of one of the DAT-independent QTLs originally mapped to mouse chromosome four. We used a combination of recombinant progeny testing and next generation sequencing to narrow the confidence interval and then identify a point mutation in the adhesion G protein-coupled receptor (aGPCR) *Bai2*. We report a missense mutation in the extracellular GPCR autoproteolysis inducing (GAIN) domain of Bai2 (Arac et al. 2012), which results in strongly reduced surface expression in heterologous cells. Our findings provide further support for a role for Bai2 in brain function, and provide insights into a possible cell biological mechanism underlying the behavioral phenotype resulting from the ENU mutagenesis.

Materials and Methods

Animals and recombinant progeny testing

All animal use was approved by the institutional animal care and use committee in accord with the guidelines laid out by the US Public Health Service. Animals were group-housed in a climate controlled facility on a 12-hour light/dark cycle (lights on at 07:00). Food (Picolab Rodent Diet 20 #5053, Lab Diet) and water were available ad libitum.

For recombinant progeny testing, N2 backcross generation recombinant males (M98 and S98) were backcrossed repeatedly to C57BL/6J females to produce large cohorts of animals for locomotor phenotyping. Subsequent recombinant progeny testing was performed similarly using recombinant males (Z49 and S49) from the N3 generation derived from the M98 lineage. The finished 4XD congenic strain was derived from the S49 lineage, using a marker-assisted breeding approach (Wakeland et al. 1997). The 4XD congenic boundaries of mutagenized DBA/2J genome introgressed onto C57BL/6J are defined by recombinations between the proximal markers D4Mit336 and 4-12891 and the distal markers mCV22652482 and mCV23567530, resulting in an introgressed region of no less than 2.1 Mb and no more than 5.1 Mb. The 4XD congenic line has been cryopreserved at the U.C. Davis Mouse Biology Program.

The allele name *Adgrb2*^{m1Djs} has been designated for the C→T transition at chr4:129686542 (NCBI Build 37, mm9) which changes an arginine residue to a tryptophan at residue 619 (R619W) in the GAIN domain encoding region of the *Bai2* gene.

Locomotor activity testing of Chromosome 4 ENU-mutagenized mice

On the testing day, 8 week old mice were transported to the testing room between the hours of 0900 and 1100 and were habituated for two hours. Locomotor activity was assayed using infrared activity monitors (Accuscan, Columbus, OH) surrounding an open field of 8×8×11 inches. Distance traveled was monitored for a period of two hours. Two acrylic boxes fit inside a single Accuscan monitor, enabling us to test two animals simultaneously. Whether another animal is present in the second box affects locomotor behavior in this assay (D.J.S and A.S.P., personal observations). We found that testing two animals from different home cages in a single Accuscan monitor both reduced variability and allowed high-throughput rates. Activity monitors were themselves housed inside sound-attenuating chambers (Med-Associates) equipped with lights and fans, both of which were turned on during the testing session. Acrylic boxes were rinsed with hot water and dried and then wiped down with a solution of 2.5% glacial acetic acid between testing sessions (Speca et al. 2006).

Locomotor activity testing of *Adgrb2*$^{tm1b(KOMP)Mbp}$ animals by International Mouse Phenotyping Consortium

Locomotor phenotyping of the *Adgrb2*$^{tm1b(KOMP)Mbp}$ (*Adgrb2*^{tm1b}) allele of *Bai2* knockout mice was performed by the International Mouse Phenotyping Consortium (IMPC) according to the following protocol: https://www.mousephenotype.org/impress/protocol/81/7#Procedure. In brief, animals were habituated to the testing room for a period of 30 minutes prior to testing. Lighting in the testing room was between 150–200 lux. Locomotor activity was monitored for 20 minutes. Nine-week old *Adgrb2*^{tm1b}(−/−) male and female mice were tested separately. Locomotor activity of *Adgrb2*^{tm1b}(−/−) animals was compared to the phenotypes of a large cohort of wild-type animals generated in the course of testing many knockout lines as part of the IMPC program.

Whole exome sequencing and mutation confirmation

Genomic DNA from the 4XD congenic strain containing ≈5 Mb mutagenized DBA/2J genomic sequence (between the markers D4Mit336 and mCV23567530) and a wild-type DBA/2J control was prepared (Gentra Puregene, Qiagen) and sent to the Broad Institute for sequencing as part of the Mutant Mouse Re-sequencing Project. In brief, exome sequencing libraries were prepared using a SureSelect kit (mouse exome v.1, Agilent), and sequencing was performed on an Illumina sequencer. FASTQ files were analyzed using GATK tools (McKenna et al. 2010). Data files containing annotated SNP calls (SnpEff ver 2.0.3) (SnpEff: Genetic variant annotation and effect prediction toolbox.) and coverage statistics were generated. The single homozygous mutation call in *Bai2* was confirmed by Sanger sequencing.

Plasmids

The pJP007 vector codes for an N-terminal signal sequence (hRAGE) followed by a putative cleavage site and a FLAG epitope tag and multiple cloning site (Pang et al. 2009). The following primer sequences were used to amplify mouse *Bai2* lacking its own signal sequence: TCCGGATCCCCTGCCCCCAGTGCCTGCTCTGC and ACCTCTAGATCACACCTCTGTCTGGAAGTCGC. This product was digested and subcloned into the BamHI and XbaI sites of the pJP007 expression vector.

We tested several different splice variants of *Bai2* for expression in heterologous cells and obtained qualitatively similar results. For the experiments described here, the splice variant tested contained four thrombospondin repeats as in isoform 1 (NP_775094.2) and had an I3 loop/STR region (Kee et al. 2002) corresponding to isoform 2 (NP_001186625.1).

An R619W mutant version of this plasmid (numbering based on the amino acid sequence of isoform 1) was created by site-directed mutagenesis (QuikChange II XL, Agilent) using the following primers: GCAGGAGCTACTGGCATGGCGCACTTACTACAGC and GCTGTAGTAAGTGCGCCATGCCAGTAGCTCCTGC.

Cell culture and transfection

All cell lines were grown in a humidified incubator at 37°C and 5% CO2. COS-1 cells (ATCC CRL-1650) were maintained in Dulbecco's modified Eagle's medium (Gibco cat # 11995-065) supplemented with 10% bovine calf serum (HyClone cat# SH30072.03), 1% penicillin/streptomycin, and 1× GlutaMAX (Thermo Fisher Scientific). HEK293T cells were maintained similarly but in medium containing Fetal Clone III serum product (Hyclone cat # SH30109.03) instead of bovine calf serum (DuBridge et al. 1987). Cells were split and seeded onto poly-l-lysine coated coverslips in 35 mm petri dishes at 10% confluence and then transfected in Opti-MEM (Thermo Fisher Scientific) 24 hours later with 1 μg of the appropriate plasmid construct using LipofectAMINE 2000 (Thermo Fisher Scientific) according to the manufacturer's protocol. Media was replaced 4 hours after transfection. Cells were grown for 40–48 hours post-transfection.

Immunofluorescence immunocytochemistry

In brief, we performed live cell labeling of the cell surface population of Bai2, after which the cells were fixed, permeabilized and subsequently labeled for total cellular population of Bai2. Specifically, coverslips were washed twice with chilled DPBS (137 mM NaCl, 2.7 mM KCl, 10 mM Na_2HPO4, and 1.76 mM KH_2PO4, pH 7.4) containing 1 mM $CaCl_2$ and 1 mM $MgCl_2$. Cells were then blocked for 15 minutes with ice-cold BSA-DPBS (2 mg/ml added bovine serum albumin). Coverslips were then incubated with primary antibody (mouse monoclonal M2 anti-FLAG antibody Sigma Cat# F3165 RRID: AB_259529; 1.0 μg/ml) in BSA-DPBS on ice for 20 minutes, after which the coverslips were washed four times with BSA-DPBS. Primary antibody bound to cell surface Bai2 was labeled with goat anti-mouse IgG1 Alexa 555 secondary antibody (ThermoFisher Scientific Cat# A21127 RRID: AB_2535769; 1:2,000). Cells were washed four times with BSA-DPBS and then fixed in a freshly made solution of 4% formaldehyde, prepared from paraformaldehyde powder (J.T. Baker) for 30 minutes. Cells were then permeabilized and blocked for 30

minutes using DPBS containing 4% w/v nonfat dry milk powder and 0.1% v/v Triton X-100. To stain for total Bai2 expression, coverslips were incubated overnight with primary rabbit anti-FLAG polyclonal antibody (Sigma-Aldrich Cat# F7425 RRID: AB_439687; 0.8 μg/ml) at 4 ° C, followed by a one-hour room temperature incubation with goat anti-rabbit IgG (H +L) Alexa 488 secondary antibody (ThermoFisher Scientific Cat# A11008 RRID: AB_143165; 1: 2,000). Nuclei were labeled using Hoechst 33258 stain (H21491; ThermoFisher Scientific). Coverslips were washed again in DPBS and mounted using Prolong Gold (P36930; ThermoFisher Scientific). Images were acquired using an AxioCam HRm high resolution CCD camera installed on an AxioObserver Z1 microscope with a 63×, 1.3-numerical aperture (NA) lens or a 20×, 0.8-NA lens and an Apotome controlled by Axiovision software (Carl Zeiss). Images were processed identically in Photoshop to maintain consistency between samples.

Immunoblot

Cell lysates were prepared as described previously (Shi et al. 1994). Proteins were separated by 3–8% SDS-PAGE (ThermoFisher Scientific cat # EA0375) and transferred to a nitrocellulose membrane. The blot was probed overnight at 4 °C with mouse anti-FLAG (Sigma Cat# F3165 RRID: AB_259529; 2.0 μg/ml) and with rabbit anti-actin (0.1 μg/mL, RRID: AB_630834, Santa Cruz Biotechnology #sc-1616R) in TBS containing 4% w/v nonfat dry milk powder and 0.1% v/v Tween 20. After three washes with TBST, the immunoblot was incubated with the appropriate HRP-conjugated secondary antibody for 60 minutes at room temperature, followed by three additional washes in TBST and incubation with ECL reagent (Advansta cat # K-12045) and exposure to x-ray film.

Scoring of expression

The percent of transfected cells was determined by counting the number of cells positive for total Bai2 immunolabeling (in the 488 channel) out of 200 total cells, as defined by Hoechst-stained nuclei, from four to six independent experiments.

Surface expression was scored in two different ways. Live surface labeling of mock transfected cells had very little background, allowing sensitive detection of very low expression levels (D.J.S, personal observation). For each scoring method, the denominator was 100 cells that exhibited total Bai2 immunolabeling performed after permeabilization (in the 488 channel). In scoring method #1 (“any”), the numerator represents the number of cells with any surface expression above background (i.e., Bai2 immunolabeling prior to permeabilization, in the 555 channel). In scoring method #2 (“hi”), the numerator represents only the number of cells that had medium (i.e., indistinguishable from wild-type) or higher levels of Bai2 cell surface immunolabeling in the 555 channel. Scoring of cell surface expression was performed in four to six independent experiments for each cell line.

Statistics

GraphPad Prism (version 5.00) was used for statistical analysis. The statistical test used for each experiment is indicated in the figure legends.

Results

A semi-dominant QTL for locomotor activity was mapped to the medial portion of mouse chromosome 4 in pedigree number 98 (Family 98) (Speca et al. 2006). Because the locus mapped equally well on both the sensitized DAT background and a wild-type background, this suggested that there was not a synergistic interaction with the DAT, and for fine-mapping it was possible to dispense with the DAT background. Random ENU mutations had been introduced on the DBA/2J (D2) strain and mutagenized mice were backcrossed to the C57BL/6J (B6) strain for phenotyping. We employed a modified recombinant progeny testing strategy to narrow the initial confidence interval. A standard recombinant progeny testing approach would first capture the QTL from one strain and backcross it completely for 10 generations onto the other strain and then narrow the QTL boundaries by making a series of sub-congenic lines and phenotyping their progeny (Fehr et al. 2002). Rather than backcross fully to the C57BL/6J strain, we phenotyped chromosome 4 recombinants as we were backcrossing to generate a congenic line. Fig. 1a shows an abbreviated pedigree of Family 98 and the lineage of the male animals used for recombinant progeny testing. The left side of Fig. 1b shows the haplotype structure of these males with recombinations in the medial portion of mouse chromosome 4. These animals were backcrossed repeatedly to C57BL/6J females and the male progeny were phenotyped for cumulative locomotor activity over a two-hour period, the same assay used for initial QTL mapping. The results and analysis of this experiment are shown on the right of Fig. 1b, where we compared the average locomotor activity of animals that were wild-type (B6B6) across chromosome 4 to animals that had the same haplotype structure as its parent (B6D2). The M98 line established a defined interval of 17.0 Mb. Negative results from the S98 and Z49 progeny testing experiments suggested a strikingly small interval of 1.4 Mb between the 4-12886 and mCV22652482 markers. Somewhat surprised by these negative data, we tested the S49 line, derived from the M98 parent, and confirmed that the phenotype was intact. Ultimately we used a marker-assisted breeding approach (Wakeland et al. 1997) to produce the 4XD congenic line through the M98/S49 lineage, encompassing an interval in between the D4Mit336 and mCV23567530 markers.

The 4XD congenic line, harboring a chromosomal region of the mutagenized D2 strain no more than 5.1 Mb, was fully backcrossed onto the B6 strain. Carriers were intercrossed and tested for locomotor activity. Both male and female mice were tested. The results of locomotor activity testing are shown in Fig. 2. Mice were phenotyped using the identical behavioral assay and same conditions as used in the original forward mutagenesis screen, although activity for only the first 20 minutes is plotted here. We observed a significant increase in cumulative distance traveled in 4XD homozygous carriers (D2D2) compared to wild-type (B6B6) or heterozygous carriers (B6D2) (Figs. 2b and 2e). However, on this uniform C57BL/6J genetic background, the heterozygous (B6D2) carriers did not have significantly elevated locomotor activity relative to wild-type (B6B6) littermates (Figs. 2b and 2e). Notably, the locomotor hyperactivity we observed in the 4XD line is quite comparable to the phenotype of a *Bai2* knockout line (*Adgrb2*$^{tm1b(KOMP)Mbp}$) characterized by the International Mouse Phenotyping Consortium (IMPC) (reproduced in Figs. 2c and 2f) (IMPC *Adgrb2* locomotor behavior URL).

Whole exome sequencing (WES) was performed on genomic DNA from homozygous carriers of the 4XD congenic line and a wild-type DBA/2J control through the Mutant Mouse Resequencing Program employing the Genome Analysis Toolkit (McKenna et al., 2010). The markers D4Mit336 and mCV23567530 define the maximal outer boundaries of the introgressed mutagenized DBA/2J chromosome spanning ≈5 Mb. The exome capture array had 718 elements within this region, which accurately reflects the number of exons. Minimum sequence coverage of target capture regions was 95.3% (>5×), 68.2% (>20×), and 35.7% (>40×). Bioinformatic analysis detected a single mutation, a C→T transition, in the GAIN domain encoding region of the *Bai2* gene (mm9; chr4:129686542), which changed an arginine residue to a tryptophan at residue 619 (R619W). This mutation was confirmed by Sanger sequencing of genomic DNA from another animal from the 4XD congenic line (Fig. 3a). Because this line had been maintained for several years, we wondered whether this mutation could have occurred spontaneously sometime after the original screen. To control for this, we performed RT-PCR followed by Sanger sequencing on total RNA from an animal that had been generated early in the screening process, and we confirmed the existence of the C→T mutation, proving that this mutation had not occurred spontaneously during the backcrossing process (D.J.S, unpublished observations). In the original screen, we had mapped this hyperactivity locus on both a wild-type background (DAT +/+) and a sensitized background (DAT +/−) (Fig. 3b). Because we generated qualitatively similar significant LOD scores on both genetic backgrounds, the evidence argues against a direct interaction with the DAT. The mutation in *Bai2* was detected close to the peak LOD scores for both genetic backgrounds (Fig. 3b).

Bai2 is a member of the adhesion GPCR (aGPCR) subfamily of receptors, defined as containing a large extracellular N-terminal domain that is often cleaved at the GPCR proteolysis site (GPS). This cleaved fragment typically remains associated with its C-terminal seven pass transmembrane (7TM) domain (Langenhan et al. 2013; Langenhan et al. 2016). The R619W mutation is located in the GAIN domain, a domain which when mutated in other aGPCRs leads to altered intracellular trafficking and reduced cell surface expression of the receptor (Arac et al. 2012; Jin et al. 2007). Thus, we performed a series of experiments to determine whether expression of Bai2 was altered in R619W mutant constructs. Because expression patterns can vary from one cell line to another, we performed experiments in two different cell backgrounds, African green monkey fibroblast COS-1 cells, and human embryonic kidney HEK293T cells. We found that in both COS-1 cells (Fig. 4) and HEK293T cells (Fig. 5) that the overall transfection efficiency and total protein expression levels of the Bai2 R619W mutant were indistinguishable from wild-type Bai2. However, we found a large and significant decrease in the cell surface expression of the R619W mutant relative to wild-type Bai2 in both cell backgrounds (Figs. 4, 5). In both COS-1 and HEK293T cells, the mutant phenotype was especially pronounced in those cells with a higher level of expression (Figs. 4, 5). These results suggest that the reduced cell surface expression of the R619W mutant GPCR that is present in these ENU-mutagenized mice may cause a loss of Bai2 function that contributes to their behavioral phenotype.

Discussion

Inspired in part by scores of groundbreaking forward mutagenesis screens in invertebrate model systems, we performed an ENU mutagenesis screen for hyperactivity in mice in the hope of identifying strong enhancers of dopaminergic neurotransmission with Mendelian patterns of inheritance that were easy to map and clone. Instead, we mapped numerous loci that influenced locomotor activity in a continuous, quantitative fashion (Speca et al. 2006).

With this study, we have now successfully identified the causative mutations for two of the semi-dominant (heterozygous) loci that we mapped, both of which act independent of the sensitized DAT background. One QTL mapped to the distal portion of mouse chromosome 12. Homozygous mutants were perinatal lethal, which facilitated rapid fine-mapping and positional cloning of that mutation (Speca et al. 2010). The semi-dominant QTL on chromosome 4 described here did not provide such a facile route to positional cloning. Because homozygous mutant animals lacked a strong, Mendelian phenotype, and because, at the time, next generation sequencing was not available to us, we chose to fine-map the locus using a modified recombinant progeny testing approach (Fehr et al. 2002) to narrow the interval from ≈20 Mb down to ≈5 Mb.

When whole exome sequencing became available through the Mutant Mouse Resequencing Program, the analysis identified a single R619W missense mutation in the *Bai2* gene within the critical region, which we subsequently confirmed by Sanger sequencing. We and others have had some success in combining forward mutagenesis, QTL mapping, and next generation sequencing to identify mutations in individual mouse genes that impact complex behavioral traits (Andrews et al. 2012; Funato et al. 2016; Gallego-Llamas et al. 2015; Ha et al. 2015; Hossain et al. 2016; Kumar et al. 2011; Militi et al. 2016; Simon et al. 2015), and while other approaches are also effective, there will likely be an important role for this screening approach in the future.

Behavioral phenotypes are quite malleable and dependent on genetic background (Sittig et al. 2016; Yalcin et al. 2004), and we found that to be the case here. Originally, we mapped a robust heterozygous chromosome 4 QTL on a B6D2 × B6 genetic background. By the time we had backcrossed this mutation completely onto the B6 strain, the hyperactive phenotype of the heterozygotes had largely disappeared (Fig. 2). In addition, the modified recombinant progeny testing approach that we used was hampered by the fact that the genetic backgrounds of the parent animals used for the mutagenesis were not uniform, leading to significant differences in locomotor behavior of chromosome 4 wild type (B6B6) animals, as can be seen in Figure 1. Furthermore, there remains ambiguity in the results of the S98 progeny test. With a p-value of 0.07, we scored the S98 recombinant as negative for capture of the QTL. However, had we tested a larger cohort, this may well have crossed the arbitrary threshold of significance (>0.05). If animals harboring the S98 haplotype were positive for the R619W mutation, its effects on locomotor activity might be masked somewhat by the unique genetic background of the S98 line. Alternatively, the S98 haplotype might not harbor the R619W mutation, and other strain-specific polymorphisms or ENU mutation(s) could result in increased locomotor activity on this genetic background. By the time we had performed whole exome sequencing, the genomic DNA for the S98 line had been discarded,

making it impossible to determine whether this line was positive for the R619W mutation. These data highlight the complexity of the effects of genetic background on even this relatively simple and robust assay for locomotor behavior.

Nevertheless, homozygous mutant (D2D2) animals from the 4XD congenic line displayed significantly elevated locomotor activity relative to wild-type (B6B6) littermates, particularly during the first twenty minutes of the testing period. These results were qualitatively and quantitatively similar to the phenotype of a *Bai2* allele (*Adgrb2*$^{tm1b(KOMP)Mbp}$) characterized by the International Mouse Phenotyping Consortium (IMPC *Adgrb2* locomotor behavior URL). However, a different *Bai2* allele (*Adgrb2*^{tm1Dgen}) showed no significant difference in open field activity, although the testing period for those animals was much shorter than that used here and was limited to five minutes (Okajima et al. 2011). At this point, it is unclear how Bai2 R619W mutation causes hyperactivity. However, we did not observe a synergistic interaction with the sensitized DAT background; therefore, a direct influence on dopaminergic homeostasis seems unlikely.

The Bai2 R619W mutation is located in the critical extracellular GAIN domain, a region that is a hallmark of the adhesion GPCR family. Many cancer mutations map to the GAIN domain in other Bai family receptors (Arac et al. 2012; Kan et al. 2010). Moreover, mutations in this domain frequently influence intracellular trafficking and cell surface expression of other aGPCR family members (Arac et al. 2012; Jin et al. 2007), as we have observed here for the R619W mutation in Bai2 (Figs. 4 and 5). The underlying molecular mechanism of the reduced intracellular trafficking and cell surface expression of Bai2 is not known, nor is whether the trafficking phenotype of the Bai2 R619W mutant can be rescued with pharmacological chaperones, as is the case for other aGPCR trafficking mutants (Jin et al., 2007). In the broader neurobiological context, the Bai family of receptors has recently been implicated in playing a role in synapse development and function (Bolliger et al. 2011; Duman et al. 2013; Kakegawa et al. 2015; Selimi et al. 2009). Moreover, *Bai2* mutant mice (*Adgrb2*^{tm1Dgen}) were shown to have increased hippocampal neurogenesis and were resistant to social defeat stress, consistent with an antidepressant-like phenotype (Okajima et al. 2011). Future mechanistic studies of the function of Bai2 and Bai family receptors in development and disease should provide additional insights into the role of this diverse family of aGPCRs.

Supplementary Material

Refer to Web version on PubMed Central for supplementary material.

Acknowledgments

We thank Colleen Manning and Danielle Mandikian for helpful advice on cell culture experiments and microscopy. Whole exome sequencing was performed at the Broad Center as part of the Mutant Mouse Re-sequencing Project at the Broad Institute (NHGRI). This research was supported by the State of California for medical research on alcohol and substance abuse through the University of California at San Francisco as well as grants from the Department of Defense (DAMD17-01-1-0799, A.S.P.), the NIH (R03-MH108950) and an Innovative Development Award from the U.C. Davis Academic Federation (D.J.S), and a NIH New Director's Innovator Award Program DP2 OD006479-01 (ED).

References

Andrews TD, et al. Massively parallel sequencing of the mouse exome to accurately identify rare, induced mutations: an immediate source for thousands of new mouse models. Open Biol. 2012; 2:120061.doi: 10.1098/rsob.120061 [PubMed: 22724066]

Arac D, Boucard AA, Bolliger MF, Nguyen J, Soltis SM, Sudhof TC, Brunger AT. A novel evolutionarily conserved domain of cell-adhesion GPCRs mediates autoproteolysis. EMBO J. 2012; 31:1364–1378. DOI: 10.1038/emboj.2012.26 [PubMed: 22333914]

Bolliger MF, Martinelli DC, Sudhof TC. The cell-adhesion G protein-coupled receptor BAI3 is a high-affinity receptor for C1q-like proteins. Proc Natl Acad Sci U S A. 2011; 108:2534–2539. DOI: 10.1073/pnas.1019577108 [PubMed: 21262840]

DuBridge RB, Tang P, Hsia HC, Leong PM, Miller JH, Calos MP. Analysis of mutation in human cells by using an Epstein-Barr virus shuttle system. Mol Cell Biol. 1987; 7:379–387. [PubMed: 3031469]

Duman JG, Tzeng CP, Tu YK, Munjal T, Schwechter B, Ho TS, Tolias KF. The adhesion-GPCR BAI1 regulates synaptogenesis by controlling the recruitment of the Par3/Tiam1 polarity complex to synaptic sites. J Neurosci. 2013; 33:6964–6978. DOI: 10.1523/JNEUROSCI.3978-12.2013 [PubMed: 23595754]

Fehr C, Shirley RL, Belknap JK, Crabbe JC, Buck KJ. Congenic mapping of alcohol and pentobarbital withdrawal liability loci to a <1 centimorgan interval of murine chromosome 4: identification of Mpdz as a candidate gene. J Neurosci. 2002; 22:3730–3738. [PubMed: 11978849]

Funato H, et al. Forward-genetics analysis of sleep in randomly mutagenized mice. Nature. 2016; 539:378–383. DOI: 10.1038/nature20142 [PubMed: 27806374]

Gallego-Llamas J, Timms AE, Geister KA, Lindsay A, Beier DR. Variant mapping and mutation discovery in inbred mice using next-generation sequencing. BMC Genomics. 2015; 16:913.doi: 10.1186/s12864-015-2173-1 [PubMed: 26552429]

Giros B, Jaber M, Jones SR, Wightman RM, Caron MG. Hyperlocomotion and indifference to cocaine and amphetamine in mice lacking the dopamine transporter. Nature. 1996; 379:606–612. DOI: 10.1038/379606a0 [PubMed: 8628395]

Ha S, Stottmann RW, Furley AJ, Beier DR. A forward genetic screen in mice identifies mutants with abnormal cortical patterning. Cereb Cortex. 2015; 25:167–179. DOI: 10.1093/cercor/bht209 [PubMed: 23968836]

Hossain MS, et al. Identification of mutations through dominant screening for obesity using C57BL/6 substrains. Sci Rep. 2016; 6:32453.doi: 10.1038/srep32453 [PubMed: 27585985]

IMPC Adgrb2 locomotor behavior URL. https://www.mousephenotype.org/phenoview/?gid=5997&qeid=IMPC_OFD_005_001,IMPC_OFD_007_001,IMPC_OFD_009_001,IMPC_OFD_010_001,IMPC_OFD_020_001

Jin Z, Tietjen I, Bu L, Liu-Yesucevitz L, Gaur SK, Walsh CA, Piao X. Disease-associated mutations affect GPR56 protein trafficking and cell surface expression. Hum Mol Genet. 2007; 16:1972–1985. DOI: 10.1093/hmg/ddm144 [PubMed: 17576745]

Kakegawa W, et al. Anterograde C1ql1 signaling is required in order to determine and maintain a single-winner climbing fiber in the mouse cerebellum. Neuron. 2015; 85:316–329. DOI: 10.1016/j.neuron.2014.12.020 [PubMed: 25611509]

Kan Z, et al. Diverse somatic mutation patterns and pathway alterations in human cancers. Nature. 2010; 466:869–873. DOI: 10.1038/nature09208 [PubMed: 20668451]

Kee HJ, et al. Expression of brain-specific angiogenesis inhibitor 2 (BAI2) in normal and ischemic brain: involvement of BAI2 in the ischemia-induced brain angiogenesis. J Cereb Blood Flow Metab. 2002; 22:1054–1067. DOI: 10.1097/00004647-200209000-00003 [PubMed: 12218411]

Kumar V, Kim K, Joseph C, Thomas LC, Hong H, Takahashi JS. Second-generation high-throughput forward genetic screen in mice to isolate subtle behavioral mutants. Proc Natl Acad Sci U S A. 2011; 108(Suppl 3):15557–15564. DOI: 10.1073/pnas.1107726108 [PubMed: 21896739]

Langenhan T, Aust G, Hamann J. Sticky signaling--adhesion class G protein-coupled receptors take the stage. Sci Signal. 2013; 6:re3.doi: 10.1126/scisignal.2003825 [PubMed: 23695165]

Langenhan T, Piao X, Monk KR. Adhesion G protein-coupled receptors in nervous system development and disease. Nat Rev Neurosci. 2016; 17:550–561. DOI: 10.1038/nrn.2016.86 [PubMed: 27466150]

McKenna A, et al. The Genome Analysis Toolkit: a MapReduce framework for analyzing next-generation DNA sequencing data. Genome Res. 2010; 20:1297–1303. DOI: 10.1101/gr.107524.110 [PubMed: 20644199]

Militi S, et al. Early doors (Edo) mutant mouse reveals the importance of period 2 (PER2) PAS domain structure for circadian pacemaking. Proc Natl Acad Sci U S A. 2016; 113:2756–2761. DOI: 10.1073/pnas.1517549113 [PubMed: 26903623]

Okajima D, Kudo G, Yokota H. Antidepressant-like behavior in brain-specific angiogenesis inhibitor 2-deficient mice. J Physiol Sci. 2011; 61:47–54. DOI: 10.1007/s12576-010-0120-0 [PubMed: 21110148]

Pang J, Zeng X, Xiao RP, Lakatta EG, Lin L. Design, generation, and testing of mammalian expression modules that tag membrane proteins. Protein Sci. 2009; 18:1261–1271. DOI: 10.1002/pro.136 [PubMed: 19472344]

Selimi F, Cristea IM, Heller E, Chait BT, Heintz N. Proteomic studies of a single CNS synapse type: the parallel fiber/purkinje cell synapse. PLoS Biol. 2009; 7:e83.doi: 10.1371/journal.pbio.1000083 [PubMed: 19402746]

Shi G, Kleinklaus AK, Marrion NV, Trimmer JS. Properties of Kv2.1 K+ channels expressed in transfected mammalian cells. J Biol Chem. 1994; 269:23204–23211. [PubMed: 8083226]

Simon MM, Moresco EM, Bull KR, Kumar S, Mallon AM, Beutler B, Potter PK. Current strategies for mutation detection in phenotype-driven screens utilising next generation sequencing. Mamm Genome. 2015; 26:486–500. DOI: 10.1007/s00335-015-9603-x [PubMed: 26449678]

Sittig LJ, Carbonetto P, Engel KA, Krauss KS, Barrios-Camacho CM, Palmer AA. Genetic Background Limits Generalizability of Genotype-Phenotype Relationships. Neuron. 2016; 91:1253–1259. DOI: 10.1016/j.neuron.2016.08.013 [PubMed: 27618673]

SnpEff: Genetic variant annotation and effect prediction toolbox. http://snpeff.sourceforge.net/

Speca DJ, et al. Conserved role of unc-79 in ethanol responses in lightweight mutant mice. PLoS Genet. 2010; 6doi: 10.1371/journal.pgen.1001057

Speca DJ, Rabbee N, Chihara D, Speed TP, Peterson AS. A genetic screen for behavioral mutations that perturb dopaminergic homeostasis in mice. Genes Brain Behav. 2006; 5:19–28. DOI: 10.1111/j.1601-183X.2005.00127.x [PubMed: 16436185]

Wakeland E, Morel L, Achey K, Yui M, Longmate J. Speed congenics: a classic technique in the fast lane (relatively speaking) Immunol. Today. 1997; 18:472–477.

Yalcin B, et al. Genetic dissection of a behavioral quantitative trait locus shows that Rgs2 modulates anxiety in mice. Nat Genet. 2004; 36:1197–1202. DOI: 10.1038/ng1450 [PubMed: 15489855]

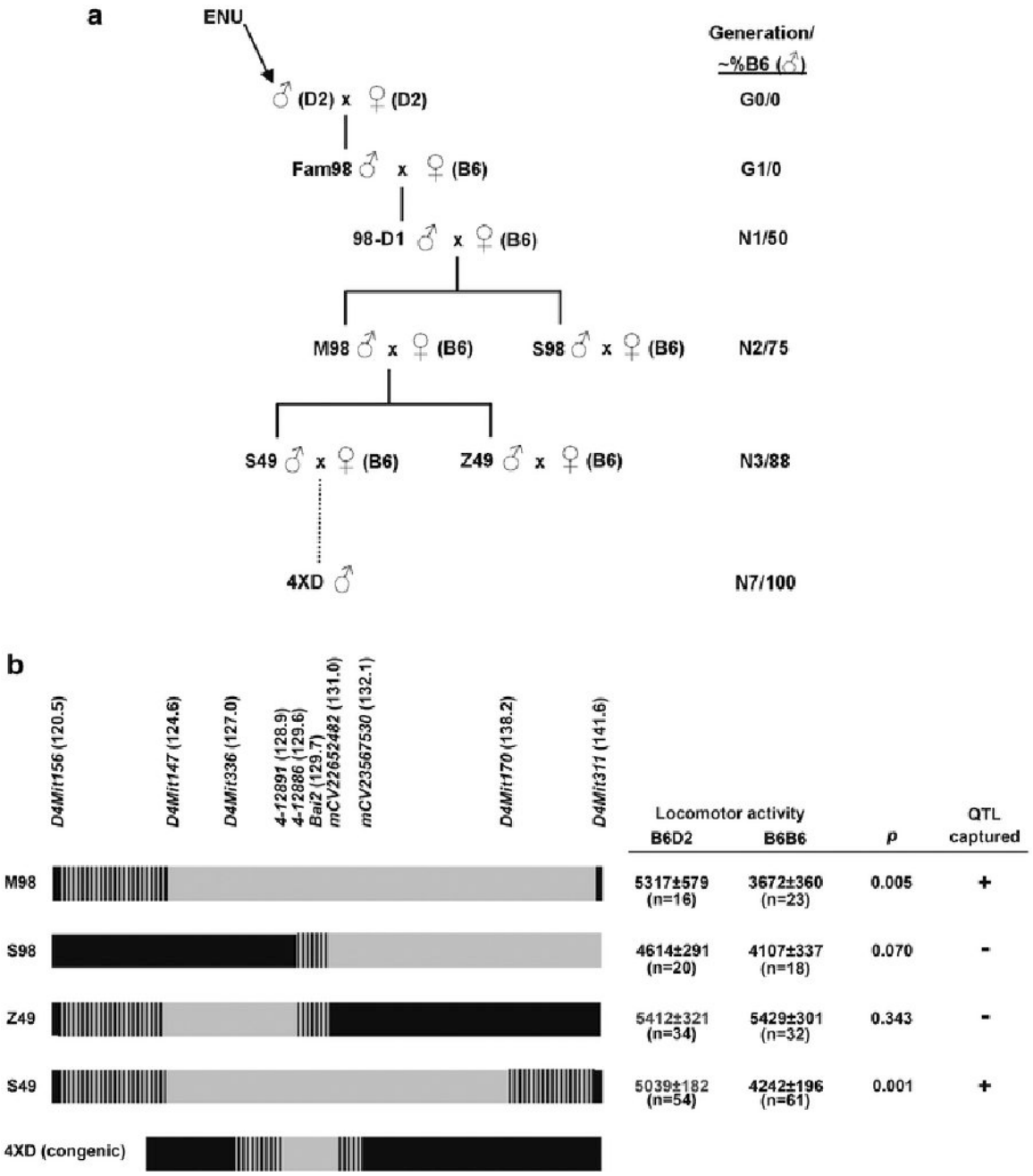

Fig 1. Fine-mapping of the semi-dominant chromosome 4 hyperactivity QTL

a Abbreviated pedigree of Family 98 showing the lineage of animals bred for recombinant progeny testing. Mouse strain is indicated in parentheses. Male animals of the D2 strain (G0) were injected repeatedly with ENU to mutagenize the germline and were bred to D2 females to fix point mutations in the G1 generation. Male founder #98 (Fam98) was crossed repeatedly to B6 female mice to generate a population of N1 animals for QTL mapping of locomotor hyperactivity, as described in (Speca et al. 2006). Statistical analysis indicated a semi-dominant QTL for hyperactivity located on chromosome 4 associated with the mutagenized D2 strain (Speca et al. 2006). Subsequent backcrossing to the B6 strain

generated male animals (M98, S98, S49, and Z49) with different recombinations within the 95% confidence interval of the chromosome 4 QTL.

b Results of recombinant progeny testing

Left, Recombinant progeny testing was performed using four male mice with recombinations within the chromosome 4 QTL. The assigned name for each mouse line is indicated on the *left*. The identity of markers used for genotyping and their mm9 positions (in megabases, shown in parentheses) are indicated at the *top*. For each mouse haplotype, the non-mutagenized B6 strain is indicated in *black*, the mutagenized D2 strain is indicated in *gray*, and indeterminate regions in between markers is indicated by the *hatched* pattern. *Right*, locomotor activity (mean + SEM, number of animals shown *below*) was measured in male mice generated from backcrossing each founder male (on the *left*) to multiple B6 females, yielding either wild-type (B6B6) or heterozygous (B6D2) progeny across the chromosome 4 region of interest. Locomotor activity was significantly higher than wild-type littermates (Mann-Whitney U test) in animals carrying the M98 and S49 haplotypes. These results led to the development of the 4XD congenic line.

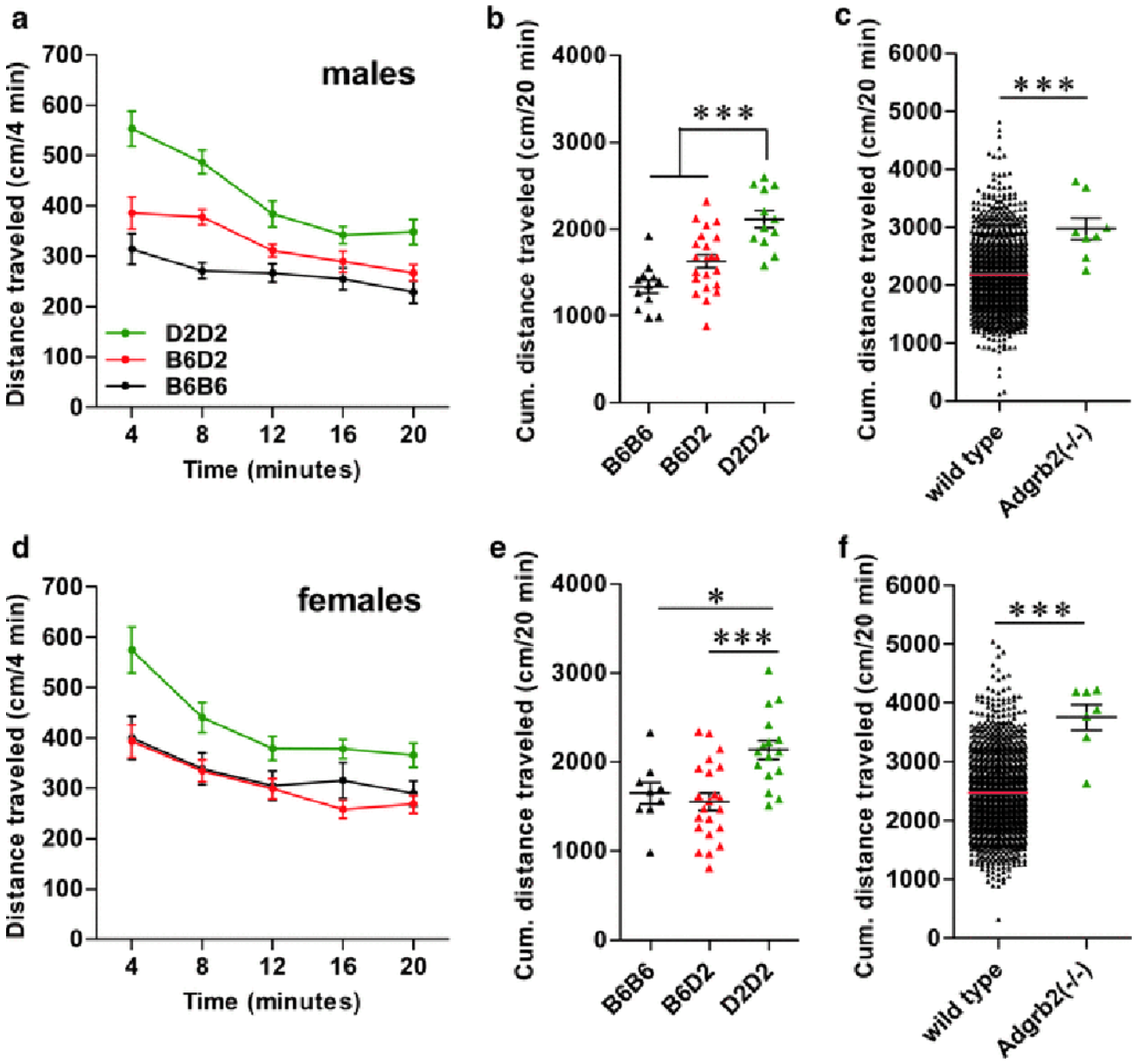

Fig 2. Capture of chromosome 4 QTL in 4XD congenic line and comparison to *Adgrb2*^{tm1b}(−/−) mice

a Distance traveled by 4XD congenic male mice over a 20-minute period. Homozygous mutant (D2D2, n=12) mice were significantly more active than heterozygous (B6D2, n=22) or wild-type (B6B6, n=12) littermates. **b** Cumulative distance traveled over a 20-minute period was significantly increased in homozygous mutant 4XD males (ANOVA with Bonferroni correction). **c** Locomotor activity of *Adgrb2*^{tm1b}(−/−) male mice (n=8) is significantly higher than wild type males (n=1,136) (Mann Whitney test). **d** Distance traveled by 4XD congenic female mice over a 20-minute period (B6B6, n=9; B6D2, n=22; D2D2, n=16). **e** Cumulative distance traveled over a 20-minute period was significantly increased in homozygous mutant 4XD females (ANOVA with Bonferroni correction). **f** Locomotor activity of *Adgrb2*^{tm1b}(−/−) female mice (n=7) is significantly higher than wild

type males (n=1,148) (Mann Whitney test). ***, $P < 0.001$; *, $P < 0.05$. Data are presented as means ± SEM. Data in **c** and **f** are reproduced with permission from the International Mouse Phenotyping Consortium (IMPC).

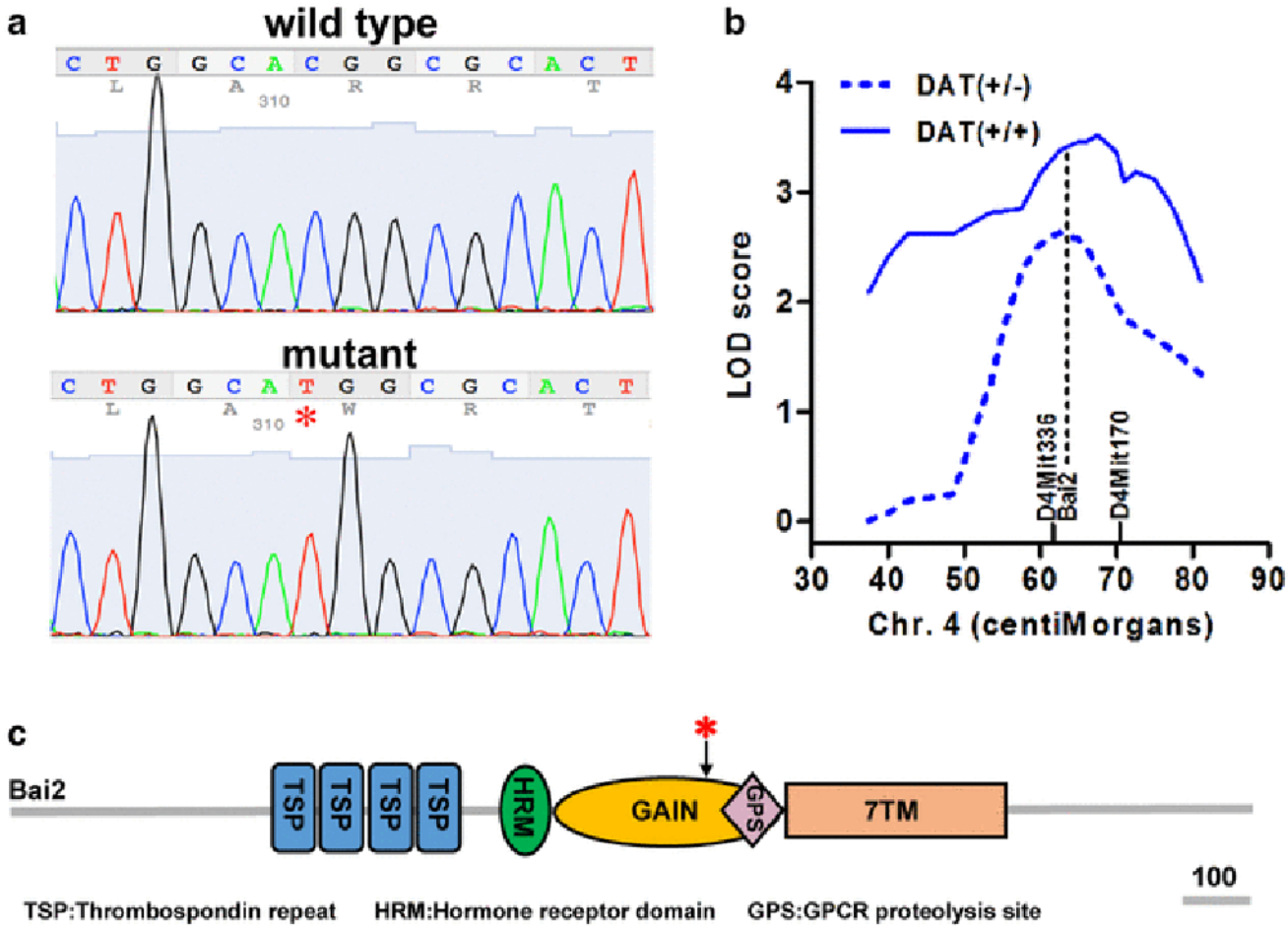

Fig 3.

Identification of *Bai2* R619W mutation

a Direct sequencing of the *Bai2* gene identified a cytosine (C)-to-thymine (T) substitution present in hyperactive 4XD congenic animals that was not present in the background D2 strain (or the B6 reference strain), highlighted by red asterisk. **b** Location of the *Bai2* gene and flanking markers superimposed on the original QTL results. QTL mapping was performed on two different genetic backgrounds: dopamine transporter wild-type (DAT(+/+)) and dopamine transporter heterozygous (DAT(+/−)). Similar LOD scores for the two genetic backgrounds suggest that the R619W mutation acts *independent* of DAT background. Data for this figure was reproduced with permission from (Speca et al. 2006) **c** Schematic diagram of the Bai2 gene product showing approximate location of the R619W mutation in GAIN domain (red asterisk). Legend bar shows length of 100 amino acids.

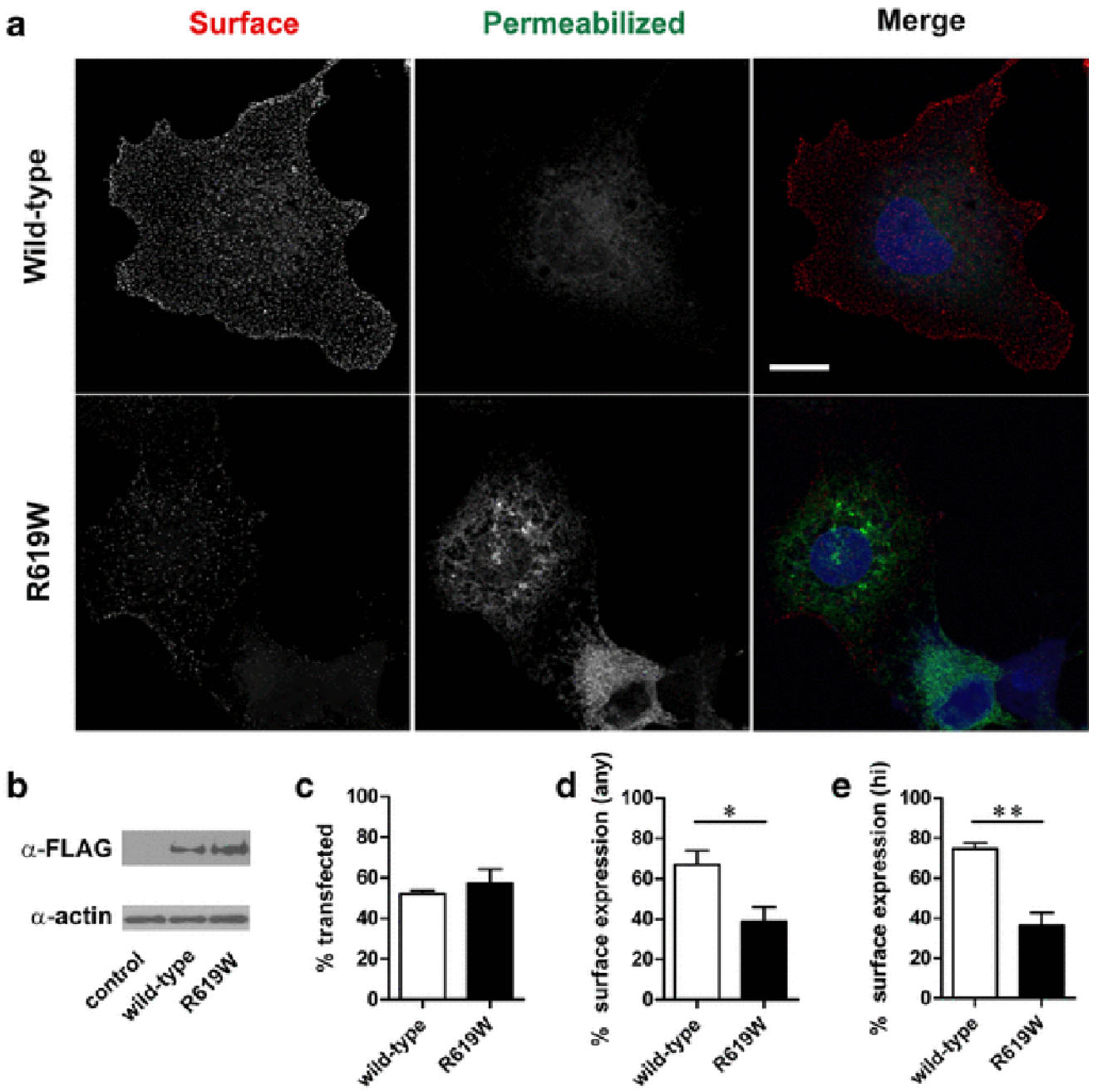

Fig 4. Reduced cell surface expression of Bai2 R619W in COS-1 cells

a Imaging of multiplex immunofluorescence-labeled cells for cell surface Bai2 (red), total Bai2 (permeabilized, green) and Hoechst 33258 (blue, to label nuclei), indicating reduced cell surface expression of Bai2 R619W. Scale bar, 10 μm. **b** Immunoblot of Bai2 wild-type and R619W demonstrating similar total expression levels. **c** Similar transfection efficiencies of Bai2 wild-type and R619W, as determined by total Bai2 immunolabeling. **d** Significantly lower cell surface expression of Bai2 R619W compared to wild-type Bai2 (scoring for any cell surface immunolabeling above background). **e** Significantly lower cell surface expression of Bai2 R619W compared to wild-type (scoring only for cells for high cell

surface immunolabeling). Values represent the combined results of four to six experiments and indicate mean ± SEM. *, $P < 0.05$, **, $P < 0.01$, by Paired t-test.

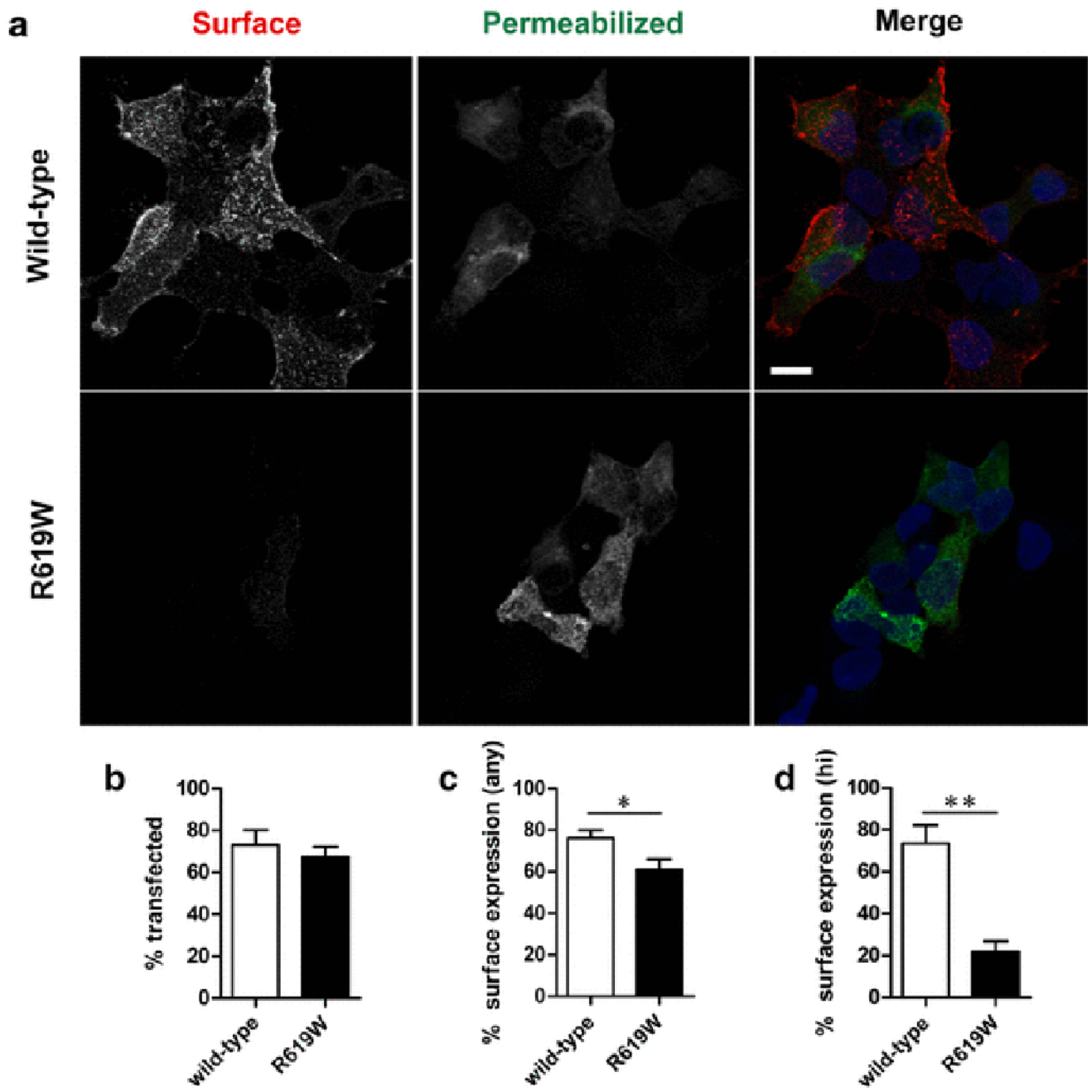

Fig 5. Lower surface expression of Bai2 R619W in HEK293T cells

a Multiplex imaging of surface Bai2 (red), total Bai2 (permeabilized, green) and Hoechst 33258 (blue, to label nuclei), indicating reduced cell surface expression of Bai2 R619W. Scale bar, 10 μm. **b** Similar transfection efficiencies of Bai2 wild-type and R619W, as determined by total Bai2 immunolabeling. **c** Significantly lower cell surface expression of Bai2 R619W compared to wild-type Bai2 (scoring for any cell surface immunolabeling above background). **d** Significantly lower surface expression of Bai2 R619W compared to wild-type (scoring for high cell surface immunolabeling). Values represent the combined

results of four to six experiments and indicate mean ± SEM. *, $P < 0.05$, **, $P < 0.01$, by Paired t-test.